RESEARCH PAPER

Conversion of Gas-Solid Reactions of the Flat Plate Particles with Unchanged Size Using the Shrinking Core Model

Ehsan Zangooei, Mohammad Reza Talaghat*

Department of Chemical, Oil and Gas Engineering, Shiraz University of Technology

Abstract

In this paper, a mathematical model is developed to calculate the conversion and the residence time reaction for plug flow and mixed flow in the fluidized reactors filled with flat plate particles using the shrinking core model. In this modeling, the size of the particles is unchanged during the reaction. Also, the reaction rate is controlled by the gas layer resistance, the ash layer resistance, and the reaction resistance as well as the combination of them. It is also assumed that the gas diffuses from the side, whereas the effect of diffusion in the axial direction is neglected. Equations are solved by numerical methods. This paper's innovation is investigating the combination of resistances effect on the conversion of the reaction. The results for a specific time show that when the reaction rate is controlled by each of the resistances individually, the conversion rate is greater. For example when the reaction is controlled by the ash layer resistance versus when the other two resistance regimes control it. Finally, the effect of the combination of different controlling regimes on the conversion and residence time of reaction for plug flow and mixed flow of particles is studied and it is found that the overall results are similar to each other. In addition, the results that the curves for the gas film layer resistance and the chemical reaction resistance, are the same and correspond to each other. Because the equations of the conversion rate are the same.

Introduction

They are of particular importance in many chemical industries where the process of solid-gas reactions takes place. Therefore, these reactions have been extensively studied and researched. In these reactions, the progress of the reaction over time depends on various factors, including the shape of the body and the type of particle flow into the reactor, and other factors [1]. In many chemical industry processes, such as combustion of solid fuel, refining of metal, and the environment, solid-gas reactions are part of these processes. [1-4]. The solid in solid-fluid reactions may be non-porous or porous. The reaction of non-porous solids was divided into three types of geometric groups [5-7]. Many interrelated mechanisms or steps characterize chemical reactions between gases and porous solids. The combination of these mechanisms and the interactions between them give rise to an overall reaction. A solid-gas reaction takes place under several stages. These steps are [8]:

1. Gaseous substance mass transfer from the bulk gas phase to the external solid surface.
2. Diffusion through a porous solid material by the gas reactant

---

* Corrresponding author:
Email: talaghat@sutech.ac.ir (M.R. Talaghat)

3. When the gaseous substance reaches the solid particle surface, it is adsorbed on its surface.
4. When the gaseous substance reaches the solid surface, then a reaction is performed on the particle's surface.
5. After reacting to the particle's solid surface, the gaseous product is desorbed from the solid particle surface.
6. The gaseous product's exit results from the reaction from inside the particle to outside it.
7. The gas product mass transfer from the outer surface of the solid particle through the GFL.

Gas – solid reactions that are exothermic or endothermic are associated with the following heat transfer steps:

I.   The direction of heat transfer inside the particle depends on whether the reaction is exothermic or endothermic.
II.   Heat transfer between the gaseous flow and the solid outer surface is convective or possibly radiant.

Various researchers have proposed different models to simulate fluid-solid reactions. One of the models used for mathematical modeling of non-porous solids is the sharp interface model, which is one of the first models used for such reactions. These models are solved analytically, the solution of which is described in standard CR engineering books [9]. In the past, solid-gas reaction models were generally considered to be dense and unstructured. Recently, however, the solid matter has been considered a porous particle in many cases. For such particles, structural parameters such as specific surface area, porosity, and pore size distribution seriously affect the rate of reaction [10]. For solid-fluid reactions that are not catalytic, two ideals models including shrinking core model (SCM) and the progressive-conversion model (PCM) are proposed [11-13].

In the PCM, the gas first enters all the particles and reacts, causing the reaction rate in different particle parts. Therefore, due to the reaction, the solid particle is consumed and turned into a product, and this action progresses throughout the particle.

SCM is used for reactions where the particle size changes significantly. SCM can be used for reactions such as solution drying, gasification, and mass burning. In these cases, the surface area of the non-reactive core particle shrinks continuously as the reaction progresses. If the particle reacts completely, all of it is consumed. With the progress of the reaction, the AL is produced by the products of the reaction. SCM for spherical particles is shown in Fig. 1.
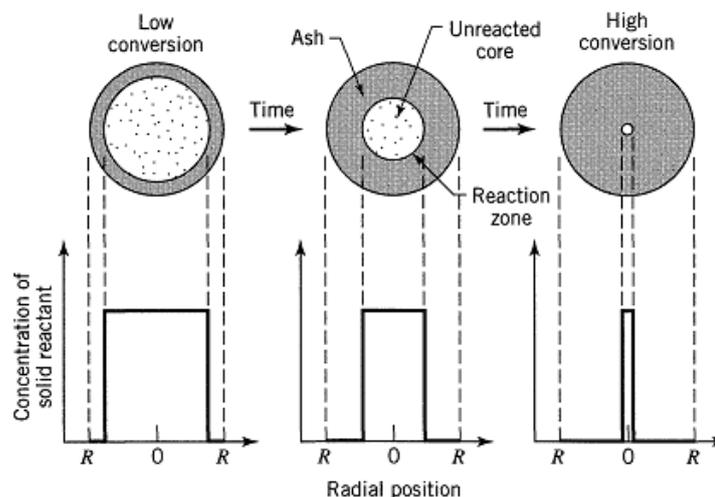
Fig. 1. The SCM for spherical particles [11]

The SCM was first presented by Yagi and Kunii [14] and then developed by Levenspiel [15] Most general fluid-solid reactions are considered as follows:

$$a_1 A_1 (gas) + a_2 A_2 (solid) \longrightarrow a_3 A_3 \ (gas) + a_4 A_4 (solid) \tag{1}$$

where a_1, a_2, a_3 and a_4 are stoichiometric coefficients.

Some fluid-solid reactions in the industry follow the shrinking core model. Some of these reactions include oxidation of ZnS [7], reduction of FeO by H_2 or CO [16], and calcination of $CaCO_3$ to form CaO. Ishida and Van [17] investigated solid-gas reactions and proposed a two-step model for these reactions. Their results show the reaction near the surface is faster than in the interior of the particle due to the propagation limitations. Szekely and Evans [18] presented the pore model. In their model, a solid was considered whose pores were parallel and whose size was equal to the particle's radius, and their distance from each other was equal. To simplify the model, they considered an incredibly thick, isothermal particle. Ramachandran and Smith [19] made a similar development. In this study, they considered pore attachment because of the expanding product. Valipour [20] modeled the non-catalytic gas-solid reaction of hematite spherical particles with synthetic gas. Rashidi et al. [21] investigated the reduction of nickel oxide with CH_4 in a calorimetric analysis. Modeling results showed that accuracy in modeling and estimation the intrinsic kinetic constant and diffusivity of product layer is necessary to consider bulk flow. Lv and Dang [22] investigated the modeling of solid-gas reactions. In this study, they examined the modeling of metal oxides reaction with CH_4 gas. Their results showed that these reactions' kinetics are consistent with the results obtained in the industrial system.

The purpose of this paper is the mathematical modeling of the calculation of the conversion and residence time of solid-gas reactions using the SCM model for flat plate particles when these solid particles flow as plug or mixed into the reactor. Several articles are available in the literature on mathematical modeling of solid-gas reactions that have been studied by researchers [23-25]. However, the following items have not been reviewed in the published articles in the literature for flat plate particles. But these items have been studied in this article and are among the innovations of this research:

i) Mathematical modeling of solid-fluid reactions when resistances combination controls the reaction rate and its influence on the reaction conversion percentage and reaction time.

ii) Influence of type of particle flow into the reactor on conversion and residence time.

Solid- gas reaction modeling

SCM model for flat plate particles with unchanging size

SCM was first introduced by Yagi and Kunii [14]. They suggested that solid-gas reactions occur in five steps using Model A. These steps can be seen in Fig. 2.

Step 1. Gaseous substance A penetrates through the GFL to reach the surface of the solid particle B.
Step 2. Gaseous substance A penetrates through the AL and reaches the surface of the unreacted core B.
Step 3. Performing a chemical reaction between gaseous substance A and a solid at the surface of a solid B (unreacted core surface)
Step 4. Emission of gaseous products resulting from the reaction through the AL to solid B's outer surface.
Step 5. Emission of gaseous products resulting from the reaction through the layer of gaseous film around the solid particle to the bulk of main gas.

In some fluid-solid reactions, some of the above steps are absent. For example, it can be seen that if the product of the reaction is only a gaseous substance, or if ash is formed, it is soft and scaly, then it causes that there is no resistance of the AL.

Eq. 2 shows a fluid-solid reaction for a solid particle that reacts with a gaseous reactant to produce the product.

$$A(gas) + B(Solid) \rightarrow Product \qquad\qquad (2)$$

A simple way to describe solid-gas reactions for solid particles is the SCM model.
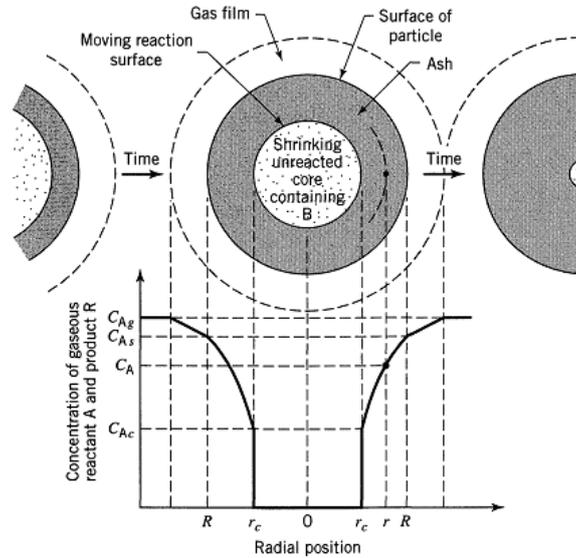
Fig. 2. Displays the concentration of reaction components in the gas- solid reaction for a spherical particle when the particle size does not change during the reaction. [11]

As shown in Fig. 3, the interface is a concentric flat plate with the outer surface for flat plate particles. In this mathematical modeling for a flat particle, it is assumed that it penetrates axially and avoid propagating in other directions.
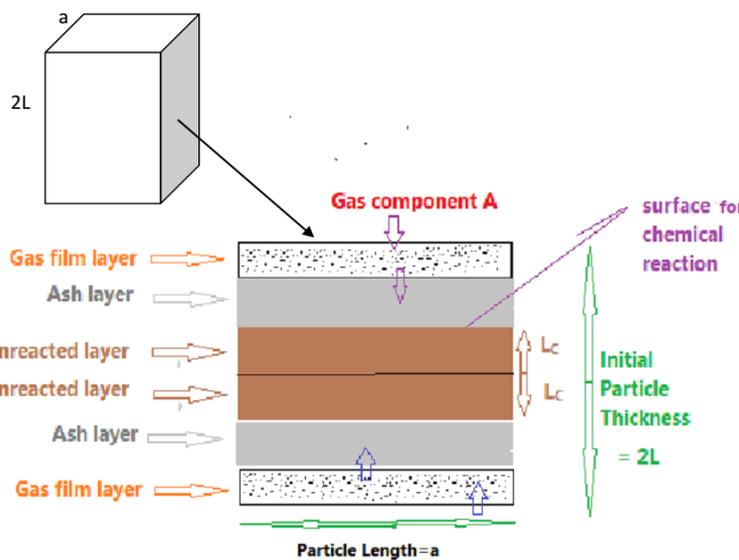
Fig. 3. Flat plate particle shape

If the particle thickness is much less than the other dimensions, the model will be more accurate. Considering the assumption causes the problem to be considered one-dimensional. One of the advantages of assuming the core-shell model for solid-gas reactions is converting each particle to the core-shell interface [1, 2].

The conversion for this model is defined as Eq. 3:

$$X_B = \frac{n_B(0) - n_B(t)}{n_B(0)} \tag{3}$$

where n_B is the solid moles number. The solid moles number ($n_B(t)$) is obtained using Eq. 4

$$n_B(t) = \frac{\rho_{Bc}}{MW_{Bc}} V_{Bc} \tag{4}$$

Finally, by combining two Eq. 3 and 4, the conversion of solid particle B is calculated using Eq. 5:

$$X_B = 1 - \frac{V_{Bc}(t)}{V_{Bc}(0)} \tag{5}$$

For this article, S_B is the area of particle surface and V_B is particle volume. In the beginning, S_B and V_B of the particle are calculated by Eq. 6 and Eq. 7. These parameters are calculated by Eq. 8 and 9 at any time of t.

$$S_B = 2a^2 \tag{6}$$
$$V_B = 2a^2L \tag{7}$$
$$S_{BC} = 2a^2 \tag{8}$$
$$V_{BC} = 2a^2L_C \tag{9}$$

where L is the half initial thickness, a is the length of the unreacted core. If Eq. 3 is written in terms of particle thickness, Eq. 10 is finally obtained.

$$X_B = 1 - \frac{L_c}{L} \tag{10}$$

Solving some fluid-solid reaction equations is not simple, so by considering several reasonable hypotheses for simplification, these reaction equations are easily solved.

There are several ways to analyze solid-gas reactions. In this study, the reaction rate-controlling step method has been used to analyze such reactions. Because the resistance of the different layers of the reaction is not the same, it is even possible that a layer's resistance is not constant during the reaction and increases or decreases as the reaction progresses. Therefore, in such cases, the most resistance step than other steps is considered the reaction rate control step.

In this study, conversion of reaction equations for flat plate particles has been developed using the following steps:

1- Penetration of gaseous substance A to the particle's solid surface through the GFL surrounds the solid particle.
2- Gaseous substance A penetrates through the AL to the unreacted core surface.
3- Carrying out a reaction between gaseous reactant A and a solid particle on its surface.

In this research, the resistance of different layers alone and a combination of these resistances are investigated. Their effects on the reaction conversion percentage and retention time are analyzed when the reaction rate is controlled by penetration through the gaseous film [1].

Controlling reaction rate by penetration of gas through the gaseous film layer

Fig. 4 shows when the gas film resistance controls the reaction rate for a spherical particle.
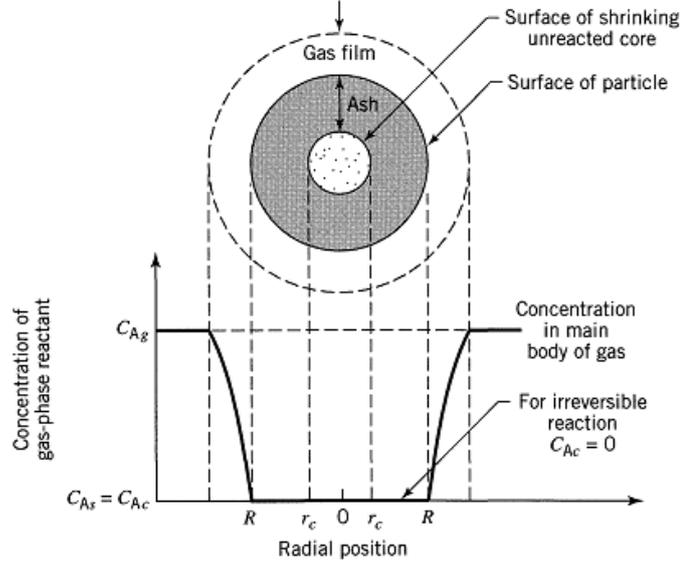
Fig. 4. Controlling reaction rate by penetration of gas through the GFL [11]

It can be seen from Fig. 4 that there is a gaseous substance A on the surface of solid particle B. Hence, the motive force of concentration equal to C_{Ag} - C_A becomes C_{Ag}. Because the gaseous reactant reacts as soon as it reaches the solid's surface and the concentration of substance A on the solid's surface becomes zero, the concentration on the solid particle surface during the reaction is constant and equal to C_{Ag}.

Since it is easier to write kinetic equations for solid-gas reactions based on the existing surface, so in the study of these reactions, attention to the stable outer surface (S_{ex}) of the solid particle B is not far from expectation.

$$dN_B = bdN_A \tag{11}$$

$$-\frac{1}{S_{ex}}\frac{dN_B}{dt} = -\frac{1}{2a^2}\frac{dN_B}{dt} = -\frac{b}{2a^2}\frac{dN_A}{dt} = bk_g(C_{Ag} - C_{As}) = bk_gC_{Ag}$$
$$= Cos(tan(t)) \tag{12}$$

where C_{Ag} and C_{As} show concentration of gas A in the gaseous phase and on the solid surface of the particle's unreacted core, k_g is the coefficient of mass transfer component A, L is half of the thickness of the flat plate, b is the coefficient between fluid and particle.

If the molar density of B is denoted by ρ_B and the volume of a particle is denoted by V, the number of mole B in a solid particle calculated by Eq. 13:

$$N_B = \rho_B V_B = (\frac{\text{moles B}}{\text{m}^3\text{solid}})(\text{m}^3 \text{ solid}) \tag{13}$$

then,

$$-dN_B = -\rho_B dV_B = -2\rho_B a^2 dL_c \tag{14}$$

The reaction rate in terms of shrinking non-reactive core thickness is obtained by substitution of Eq. 14 in Eq. 12:

$$-r_B = -\frac{1}{S_{ex}}\frac{dN_B}{dt} = -\frac{1}{2a^2}\frac{2\rho_B a^2 dL_c}{dt} = -\rho_B\frac{dL_c}{dt} = bk_gC_{Ag} \tag{15}$$

By rearranging and integrating, the time required for the non-reactive core to decrease over time is calculated by Eq. 16.

$$t = \frac{\rho_B L}{bk_g C_{Ag}} \left(1 - \frac{L_c}{L}\right) \tag{16}$$

$$\tau_f = \frac{\rho_B L}{bk_g C_{Ag}} \tag{17}$$

where L_c is half the thickness of flat plate particle relative to the origin of the coordinates which has not yet reacted. The time required for a solid particle to react completely and become a product is τ. then

$$\frac{t}{\tau_f} = 1 - \frac{L_c}{L} \tag{18}$$

The calculation of the fraction conversion can be presented using Eq. 8 as Eq. 19:

$$\frac{t}{\tau_f} = X_B \tag{19}$$

For each particular conversion in the gas-solid reactions, the required reaction time is the same for all particles when the particle flow is plugged. So, when penetrating through the GFL is the controlling step, the conversion is the same for single solid particles or many particles and is calculated using Eq. 19 [6-8, 11].

Controlling reaction rate by penetration of gas through the AL

A two-step analysis is required when the AL resistance controls the diffusion. It is assumed that the reaction is initially carried out on the outer surface and on the flat plate's two sides, according to Fig. 3. The reaction between a flat plate and a gas fluid is made under reaction 2, and the mass balance is written according to Eq. 4 for flat plate particles.

Rate disappearance=Accumulation $\hspace{6cm}$ (20)

According to Eq. 21, the reaction rate for component A at any time is equivalent to its diffusion rate toward the reaction surface.

$$-\frac{1}{s}\frac{dN_A}{dt} = Q_A \tag{21}$$

where, S is the particle flat plate external surface, Q_A is the flux of gas material A in the AL. Q_A is calculated using Fick's law as Eq. 20.

$$Q_A = D_e \frac{dC_A}{dZ} \tag{22}$$

where, D_e is the effective penetration coefficient of gaseous substance A through the AL and L is half the thickness of the flat plate-shaped at the beginning of the reaction. From the combination of Eq. 21, Eq. 22 and the Eq. 23 is obtained:

$$-\frac{1}{s}\frac{dN_A}{dt} = -\frac{1}{2a^2}\frac{dN_A}{dt} = D_e\frac{dC_A}{dZ} \tag{23}$$

In the first step, by integrating Eq. 21 through the AL and sorting it, Eq. 22 is obtained:

$$-\frac{1}{2a^2 D_e}\frac{dN_A}{dt}(L_c - L) = C_{Ag} \tag{24}$$

Using Eqs. 3 ,13 and 15, the Eq. 25 is obtained:

$$dN_A = \frac{2a^2 \rho_B dL_c}{b} \qquad (25)$$

In this case, the dN_A/dt is constant for a given size of the non-reactive core. However, when the gas-solid reaction is done and progresses, the core becomes smaller, and instead, the AL becomes thicker, eventually reducing the penetration of reactant A through the AL. Consequently, in the second stage of review and analysis, the non-reactive nucleus' size is allowed to change over time. In this case, by combining and integrating Eqs. 24 and 25, the time required for the reaction is obtained by Eq. 26:

$$t = \frac{\rho_B L^2}{2bD_e C_{Ag}} ((\frac{L_c}{L})^2 - 2\frac{L_C}{L} + 1) \qquad (26)$$

The amount of conversion of the unreacted particle B is the ratio of the unreacted particle B's volume at any time to the particle's total initial volume. Consequently, by using Eqs. 26 and 27, the conversion rate of a single flat plate particle is calculated to state that penetration through the AL controls and the particle size is constant.

$$1 - x_B = \frac{2L_c a^2}{2L a^2} = \frac{L_c}{L} \qquad (27)$$

$$X_B = (\frac{t}{\tau_A})^{0.5} \qquad (28)$$

τ_A is the time required for a solid particle to react entirely and become a product and is calculated using Eq. 29:

$$\tau_A = \frac{\rho_B L^2}{2bD_e C_{Ag}} \qquad (29)$$

For each particular conversion in the gas-solid reactions, the required reaction time is the same for all particles when the particle flow is the plug. Therefore, when diffusion through the AL is the controlling step, the conversion is the same for single solid particles or many particles and is calculated using Eq. 26 [6-8, 11].

When a single particle has a mixing flow, the particle's conversion to the product depends on residence time in each particle's bed, and this conversion is variable, and its average conversion must be calculated. The average conversion of solid particles for a mixed flow is obtained from Eq. 30.

$$1 - \overline{X}_B = \int_0^{\tau_A} (1 - X_B) E dt \qquad (30)$$

where E is the residence time distribution of the solid particles in the reactor. When the flow of solid particles into the reactor is mixed, the residence time of these solid particles is calculated by Eq. 31:

$$E = \frac{1}{\overline{t}} e^{-\frac{t}{\overline{t}}} \qquad (31)$$

Substitution of Eq. 31 in Eq. 30, the conversion of reaction for solid particles is calculated by Eq. 32 when the solid flow is mixed:

$$1 - \overline{X}_B = \int_0^{\tau_A} \frac{1}{\overline{t}} e^{-\frac{t}{\overline{t}}} (1 - X_B) dt \qquad (32)$$

Also, Replacing Eq. 28 in Eq. 32 gives:

$$1 - \bar{X}_B = \int_0^{\tau_A} (1 - (\frac{t}{\tau_A})^{0.5} \frac{1}{t} e^{-\frac{t}{t}} dt \tag{33}$$

Combination of resistances

In the above equation, it is assumed that only single resistance during the reaction is the controller. However, in solid-gas reactions, as the reaction progresses, the relative importance of the resistances, including the resistance of the GFL, the resistance of AL, and the resistance of the chemical reaction (CR), is not constant and changes. For example, for a solid particle B whose size is constant during the chemical reaction, the Resistance of GFL does not change and remains constant. By decreasing the non-reactive core surface, resistance to reaction increases. Layers' resistance during the solid-gas reaction is not constant and their importance varies during the reaction. For example, the AL resistance at the beginning of the reaction is zero because there is no ash at all, but as the reaction progresses, ash also forms, and with the creation of this layer, its importance gradually increases. Therefore, it is considered that it is not logical to consider only one stage of reaction control and a combination of resistances that depends on the type of reaction should be considered.

It is assumed that the GFL and AL resistances control the reaction rate simultaneously. Then, the time required for this gas-solid reaction is the sum of the times needed for GFL and AL resistances if it is a reaction controller alone.

$$t_{total} = t_f + t_A = \tau_f x_B + \tau_A x_B^2 \tag{34}$$

where t_f and t_A are the time required for the GFL resistance and AL resistance. Eq. 34 is calculated for a single particle and can be used for solid particles of the same size, flowing into the reactor as a plug flow.

For the mixed flow of particle, the average conversion of solids is calculated using Eq. 35:

$$1 - \bar{X}_B = \int_0^{\tau_{total}} (1 - x_B) \frac{1}{t} e^{-\frac{t_{total}}{t}} dt_{total} \tag{35}$$

τ_{total}, is the total time needed to convert the total particle, and is equal to the total contact time necessary for states that the gas layer film resistance (τ_f) and the AL resistance (τ_A) control the rate of the reaction.

$$\tau_{total} = \tau_f + \tau_A \tag{36}$$

To calculate the Eq. 35, x_B is calculated by Eq. 34. It should be noted that all equations are solved using numerical methods.

Results and discussion

In this study, solid-gas reactions are modeled using the SCM for flat plate particles when these solid particles flow as plugs or mixed into the reactor. In this mathematical modeling, the size of the particle during the reaction is constant. In this research, the control of the chemical reaction rate is investigated by each layer resistances, including resistance of GFL, AL resistance, CR resistance, and a combination of each of these resistances. The results of this study are shown in Table 1.

For evaluating the model presented in this research, the results obtained from the mathematical modeling are compared with the experimental data from the reaction of anthraquinone, and sodium sulfide is obtained in an alkaline environment available in the literature for cylindrical particles [12]. A comparison between the results of the model presented in this study and the experimental data available at various temperatures is illustrated in Fig. 5.
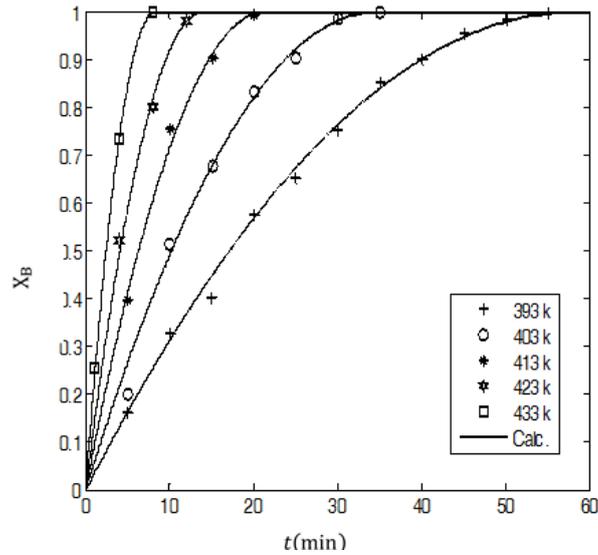
Fig. 5. Anthraquinone particles conversion at different temperatures in the fluid-solid reaction when controlling step is CR

By observing Fig. 5, it is clear that the modeling results with experimental data is a good match. According to Fig. 5, as the reaction temperature increases, the reaction conversion percentage also increases.

The results obtained for converting a flat plate particle when solid particles enter the reactor with a plug flow are shown in Fig. 6. In this case, the chemical reaction rate is controlled individually by each resistance. As can be seen from Fig. 6, for a given reaction time, when the AL resistance controls the rate of reaction, the conversion is more than when the other two resistances control the reaction rate. Observing Fig. 6 also shows that the curves related to the two resistances including the GFL and the CR are coincides because the equations related to these two resistances are the same.

In the cases studied in this research, it was assumed for flat plate particles that the rate controlling step of the solid-gas reaction is only one resistance. However, as the reaction progresses, resulting in more flat plate particle conversion of reaction, the resistances' relative importance will vary.
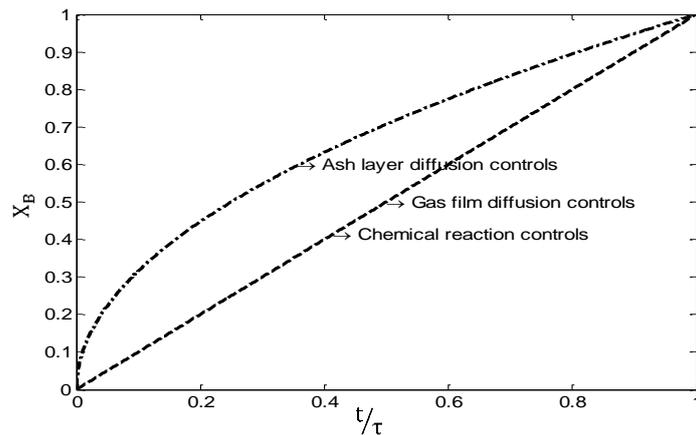
Fig. 6. Conversion reaction at different residence times for flat plate particles with plug flow in which each resistance alone controls the rate of reaction

Table 1. Conversion of reaction and residence time reaction for flat plate particles

Mixed flow	Plug flow	
$$\overline{X}_B = 1 - \int_0^{\tau_f}\left(1 - \frac{t}{\tau_f}\right)\frac{e^{-\frac{t}{\bar{t}}}}{\bar{t}}dt$$ $$\tau_f = \frac{\rho_B L}{bk_g C_{Ag}}$$	$$X_B = \frac{t}{\tau_f}$$ $$\tau_f = \frac{\rho_B L}{bk_g C_{Ag}}$$	**Gas film layer resistance**
$$\overline{X}_B = 1 - \int_0^{\tau_A}\left(1 - \left(\frac{t}{\tau_A}\right)^{0.5}\right)\frac{e^{-\frac{t}{\bar{t}}}}{\bar{t}}dt$$ $$\tau_A = \frac{\rho_B L^2}{2bD_e C_{Ag}}$$	$$X_B = \left(\frac{t}{\tau_A}\right)^{0.5}$$ $$\tau_A = \frac{\rho_B L^2}{2bD_e C_{Ag}}$$	**Ash layer resistance**
$$\overline{X}_B = 1 - \int_0^{\tau_R}\left(1 - \frac{t}{\tau_R}\right)\frac{e^{-\frac{t}{\bar{t}}}}{\bar{t}}dt$$ $$\tau_R = \frac{\rho_B L}{bk^* C_{Ag}}$$	$$X_B = \frac{t}{\tau_R}$$ $$\tau_R = \frac{\rho_B L}{bk^* C_{Ag}}$$	**Chemical reaction resistance**
$$\overline{X}_B = 1 - \int_0^{\tau_t}(1 - X_B)\frac{e^{-\frac{t_t}{\bar{t}}}}{\bar{t}}dt_t$$ $$t_t = \tau_f X_B + \tau_A X_B^2$$ $$\tau_t = \tau_f + \tau_A$$ $$\tau_A = \frac{\rho_B L^2}{2bD_e C_{Ag}} \tau_f = \frac{\rho_B L}{bk_g C_{Ag}}$$	$$t_t = \tau_f X_B + \tau_A X_B^2$$ $$\tau_f = \frac{\rho_B L}{bk_g C_{Ag}} \qquad \tau_A = \frac{\rho_B L^2}{2bD_e C_{Ag}}$$	**Combination of gas film layer resistance and ash layer resistance**
$$\overline{X}_B = 1 - \int_0^{\tau_t}(1 - X_B)\frac{e^{-\frac{t_t}{\bar{t}}}}{\bar{t}}dt_t$$ $$t_t = \tau_f X_B + \tau_R X_B$$ $$\tau_t = \tau_f + \tau_R$$ $$\tau_R = \frac{\rho_B L}{bk^* C_{Ag}} \tau_f = \frac{\rho_B L}{bk_g C_{Ag}}$$	$$t_t = \tau_f X_B + \tau_R X_B$$ $$\tau_f = \frac{\rho_B L}{bk_g C_{Ag}} \qquad \tau_R = \frac{\rho_B L}{bk^* C_{Ag}}$$	**Combination of chemical reaction resistance and gas film layer resistance**
$$\overline{X}_B = 1 - \int_0^{\tau_t}(1 - X_B)\frac{e^{-\frac{t_t}{\bar{t}}}}{\bar{t}}dt_t$$ $$t_t = \tau_A X_B^2 + \tau_R X_B$$ $$\tau_t = \tau_A + \tau_R$$ $$\tau_R = \frac{\rho_B L}{bk^* C_{Ag}} \tau_A = \frac{\rho_B L^2}{2bD_e C_{Ag}}$$	$$t_t = \tau_A X_B^2 + \tau_R X_B$$ $$\tau_A = \frac{\rho_B L^2}{2bD_e C_{Ag}} \qquad \tau_R = \frac{\rho_B L}{bk^* C_{Ag}}$$	**Combination of ash layer resistance and chemical reaction resistance**
$$\overline{X}_B = 1 - \int_0^{\tau_t}(1 - X_B)\frac{e^{-\frac{t_t}{\bar{t}}}}{\bar{t}}dt_t$$ $$t_t = \tau_f X_B + \tau_A X_B^2 + \tau_R X_B$$ $$\tau_t = \tau_f + \tau_A + \tau_R$$ $$\tau_A = \frac{\rho_B L^2}{2bD_e C_{Ag}} \quad \tau_R = \tau_f = \frac{\rho_B L}{bk_g C_{Ag}}$$ $$\frac{\rho_B L}{bk^* C_{Ag}}$$	$$t_t = \tau_f X_B + \tau_A X_B^2 + \tau_R X_B$$ $$\tau_A = \frac{\rho_B L^2}{2bD_e C_{Ag}} \tau_f = \frac{\rho_B L}{bk_g C_{Ag}}$$ $$\tau_R = \frac{\rho_B L}{bk^* C_{Ag}}$$	**Combination of gas film layer resistance, ash layer resistance and chemical reaction resistance**

In the following, the combination resistances effect on the conversion and residence time is investigated.

Fig. 7 explains the combination of two resistances effect, including the GFL resistance and the AL resistance, on the conversion for the flat-plate with plug flow when simultaneously controlling the chemical reaction. According to Fig. 7, reducing the GFL resistance and increasing the AL resistance reduces the reaction time for a specific conversion. It can also be said that by decreasing the GFL resistance and increasing the AL resistance, the conversion increases. When a hard AL develops around the particle during a gas-solid reaction as the reaction progresses, the resistance to the penetration of gas reactant A through the AL is usually greater than its penetration through the GFL around the particle.Therefore, if there is a hard AL, then the GFL resistance can be ignored.
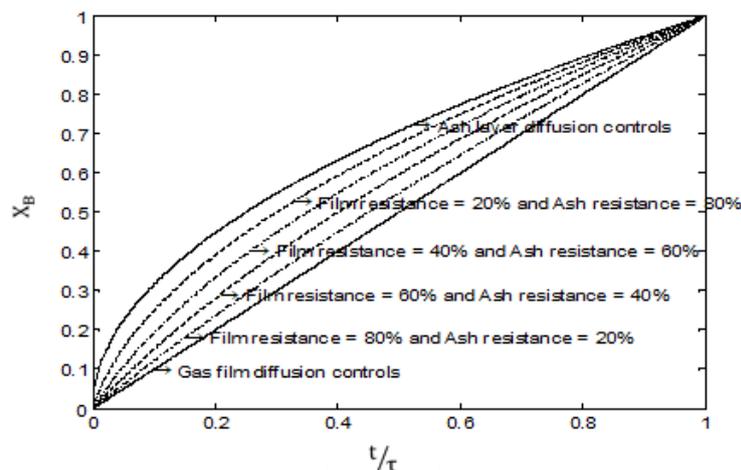
Fig. 7. Conversion reaction at various residence times for particles with plug flow, in the case of reaction rate is controlled by the GFL resistance and the AL resistance simultaneously

The study results of the resistances combination effect, including the GFL resistance and CR resistance when the flat plate particles in the reactor have plug flow, are shown in Fig. 8.
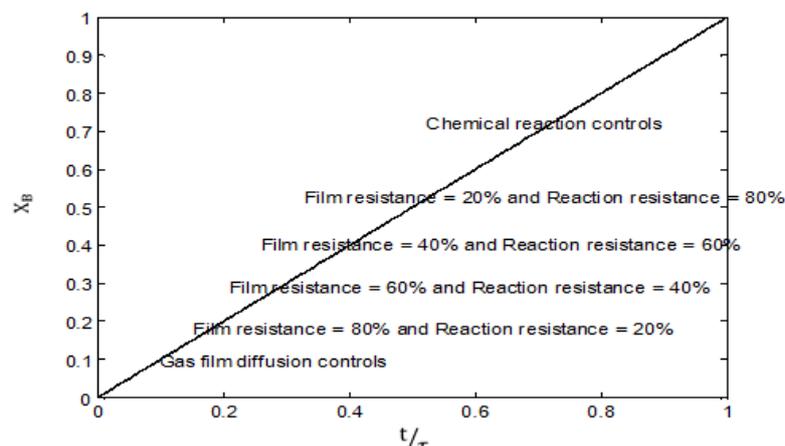
Fig. 8. Conversion reaction at various residence times for particles with plug flow, in the case of reaction rate is controlled by the GFL resistance and the CR resistance simultaneously

In this case, the CR rate is controlled simultaneously by the GFL resistance and CR resistance. As can be seen from the figure, reducing the GFL resistance and increasing the CR resistance causes the reaction time to be reduced for a given reaction conversion. Also, it can be said that for a particular time to perform the reaction, reducing the GFL resistance and increasing the CR resistance will increase the conversion percentage of the reaction.

The study results of the resistances combination effect, including the AL resistance and the CR resistance when the flat plate particles in the reactor have plug flow, are shown in Fig. 9.

In this case, the CR rate is controlled simultaneously by the AL resistance and the CR resistance. As can be seen from the figure, increasing the AL resistance and reducing the CR resistance causes the reaction time to be reduced for a given reaction conversion. Moreover, it can be said that increasing the AL resistance and reducing the CR resistance will increase the conversion percentage of the reaction for a particular time to perform the reaction.
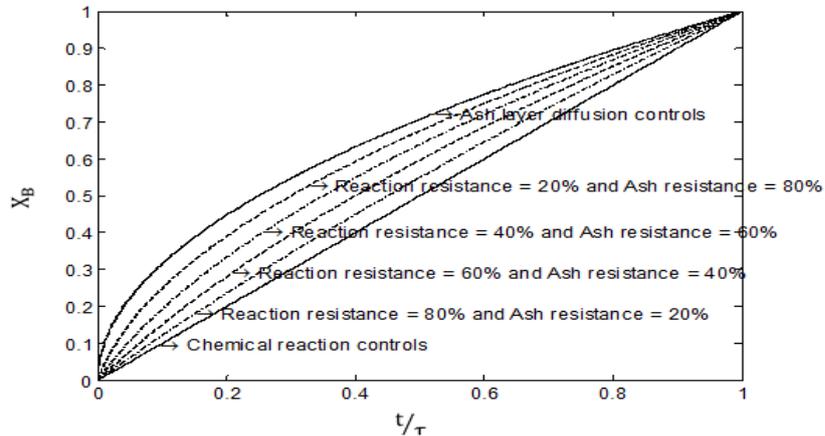
Fig. 9. Conversion reaction at various residence times for particles with plug flow, in the case of reaction rate is controlled by the AL resistance and the CR resistance simultaneously

Fig. 10 shows the three resistances combination effect, including a GFL resistance, AL resistance, and CR resistance for flat particles when particles in the reactor have plug flow.
In this case, the chemical's rate is controlled simultaneously by the GFL resistance, the AL resistance, and the CR resistance.

As can be seen from the figure, if the GFL resistance is considered constant for a specific conversion, increasing the AL resistance and decreasing the CR resistance will reduce the reaction time.
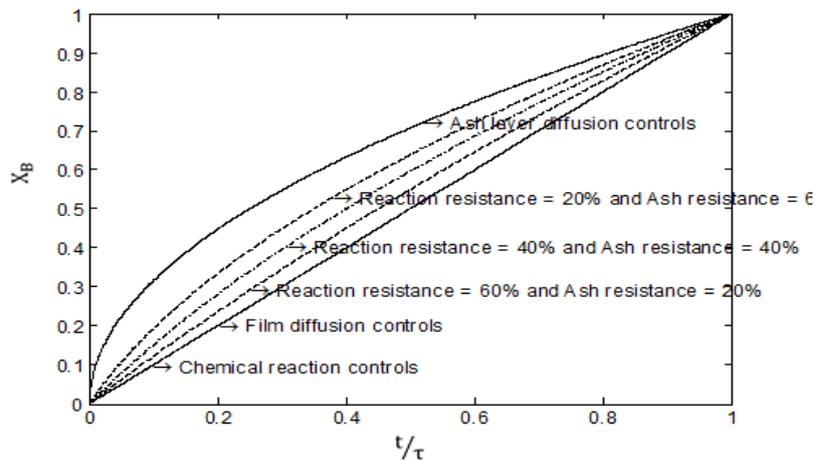
Fig. 10. Conversion reaction at various residence times for particles with plug flow, in the case of reaction rate is controlled by the GFL resistance, the AL resistance and CR resistance simultaneously

In this research, for solid-gas reactions, the effect of flat plate particle mixed-flow on the conversion percentage and reaction time was also investigated. The results of this study are as follows.

Fig. 11 shows the conversion of a solid-gas response for flat plate particles with the mixed flow in the reactor. In this study, each of the resistances alone, including the GFL resistance, the AL resistance, and the CR resistance, controlled the rate of gas-solid reaction... This figure

shows that when the AL resistance controls the reaction rate, the conversion for a specific time is more than when two other resistances control the CR rate. On the other hand, for a given conversion, the time required to perform the reaction when the AL resistance controls the reaction rate is less than when the other two regimes control the chemical reaction. It is observed that curves for the resistance of the GFL and the resistance of CR are the same, and both curves match each other because the equations of the rate of conversion are the same.

The resistances combination effect, including GFL resistance and the AL resistance for flat plate particles with mixed flow on the conversion, is illustrated in Fig. 12. In this case, the CR rate is controlled simultaneously by the AL resistance and the GFL resistance. This figure shows that increasing the GFL resistance and reducing the AL resistance causes the reaction time to be increased for a given conversion. On the other hand, for a specified time, by increasing the resistance of GFL resistance and by reducing AL resistance, the conversion reduces.
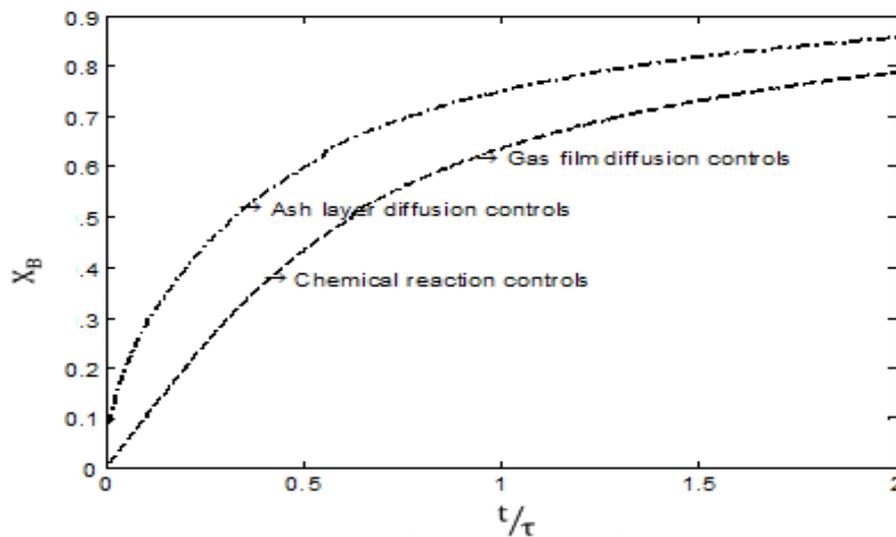
Fig. 11. Conversion reaction at different residence times for particles with mixed flow, in the case of the solid-gas CR rate is controlled by each of the resistances alone
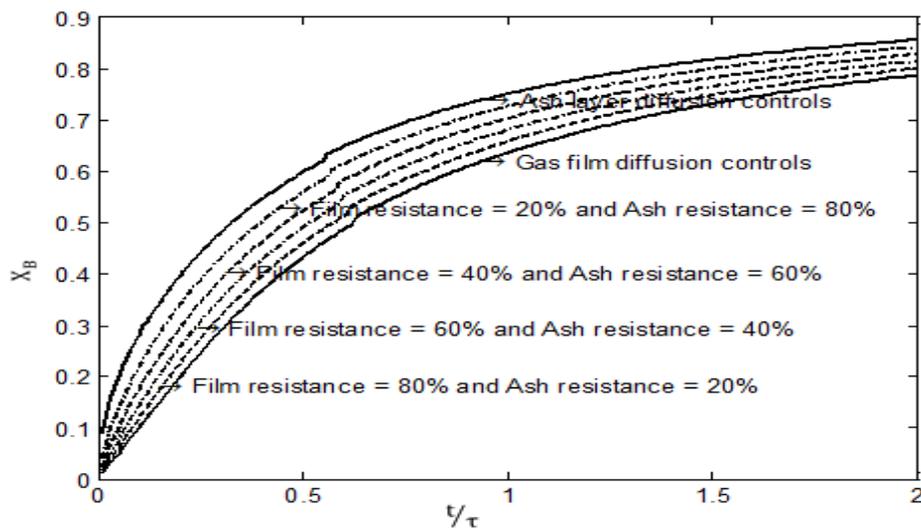
Fig.12. Conversion reaction at various residence times for particles with mixed flow, in the case of reaction rate is controlled by the GFL resistance and the AL resistance simultaneously

The resistances combination effect, including a GFL resistance and the CR resistance for flat plate particles with mixed-flow on the conversion, is shown in Fig. 13.
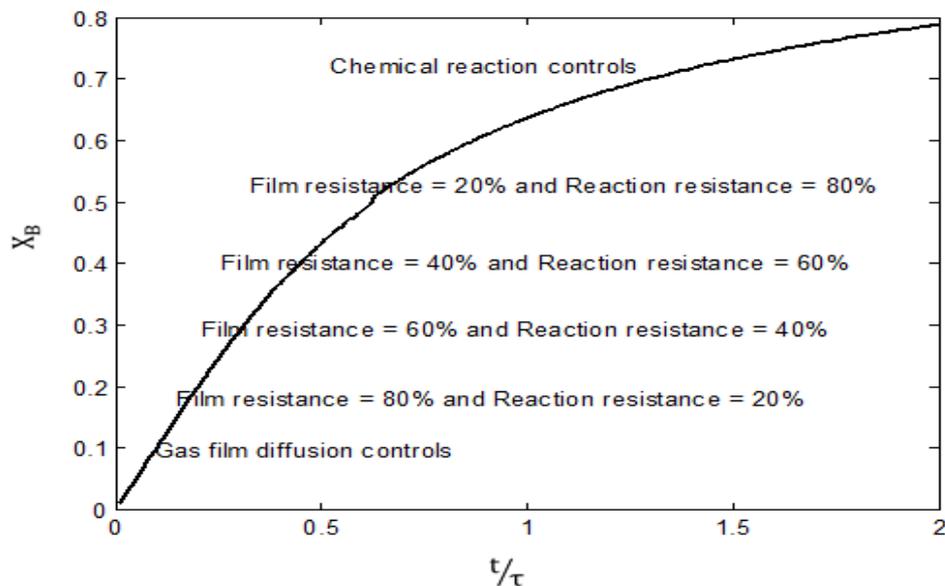
Fig. 13. Conversion reaction at various residence times for particles with mixed flow, in the case of reaction rate is controlled by the GFL resistance and the CR resistance simultaneously

In this case, the CR rate is controlled simultaneously by the GFL resistance and the CR resistance Fig. 13 show that increasing the GFL resistance and reducing the CR resistance causes the reaction time to be increased for a given conversion. Also, for a specified time, by increasing the GFL resistance and by reducing the CR resistance, the conversion reduces.

Fig. 14 explains the resistance combination effect, including the AL resistance and the CR resistance for flat plate particles with mixed flow on the conversion. In this case, the CR rate is controlled simultaneously by the AL resistance and the CR resistance. As can be seen from the figure, reducing the AL resistance and increasing the CR resistance causes the reaction time to be increased for a given conversion. Moreover, by reducing the AL resistance and increasing the CR resistance, the conversion reduces for a specified time.

Finally, Fig. 15 shows the three resistances combination effect, including the GFL resistance, the AL resistance, and the CR resistance for flat plate particles with the mixed flow in the reactor on the reaction conversion and residence time. In this case, the CR rate is controlled simultaneously by the GFL resistance, the AL resistance, and the CR resistance.

Fig. 15 shows, if the GFL resistance is considered constant for a specific conversion, reducing the AL resistance and increasing the CR resistance will increase the reaction time. Also, for a specified time, by decreasing the AL resistance and by increasing the CR resistance, the conversion reduces.
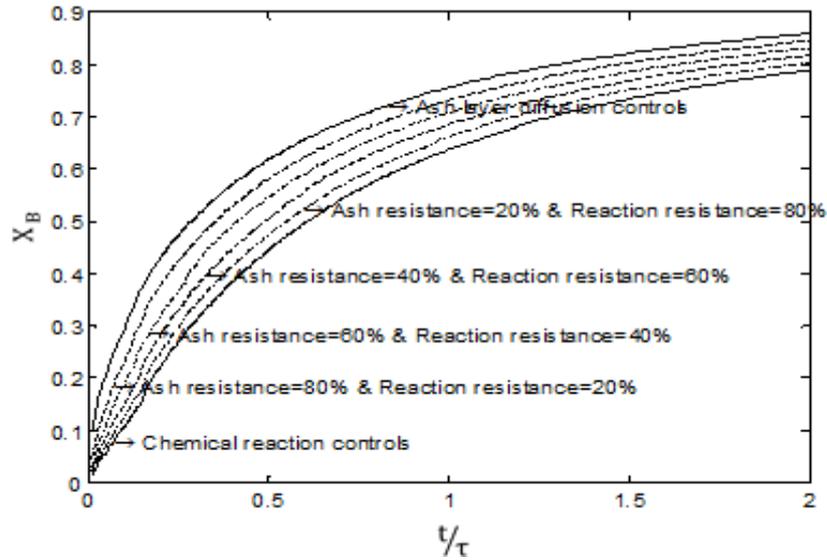
Fig. 14. Conversion reaction at various residence times for particles with mixed flow, in the case of reaction rate is controlled by the AL resistance and the CR resistance simultaneously
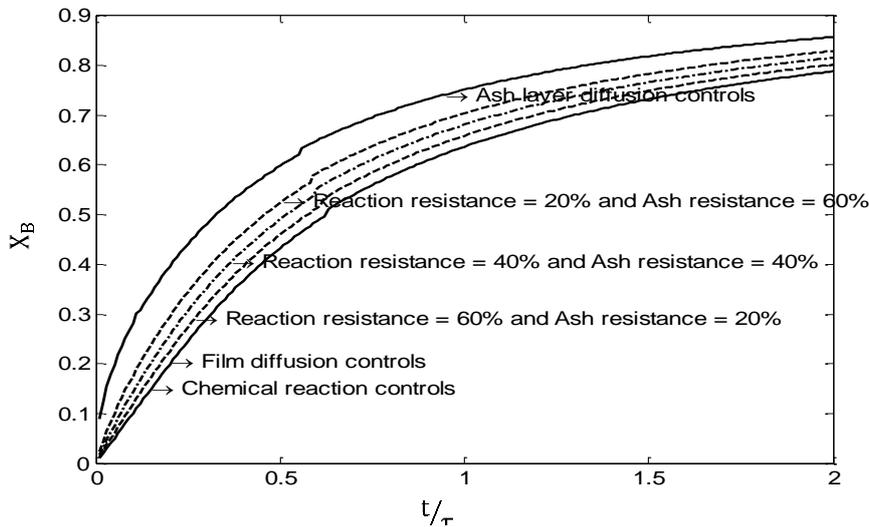
Fig. 15. Conversion reaction at various residence times for particles with mixed flow, in the case of reaction rate is controlled by the GFL resistance, the AL and the CR resistance simultaneously

Conclusion

In this study, the calculation of conversion of reaction and reaction time of solid-gas reactions is modeled using the SCM for flat plate particles when these solid particles flow as plug or mixed into the reactor.

In this modeling, the particle size during the reaction is constant. In this research, the control of the reaction rate is investigated by each layer resistances, including GFL resistance, AL resistance, CR resistance, and a combination of each of these resistances. The studies mentioned in this study are innovative and are not available in the literature. For evaluating the model presented in this research, the results of modeling and laboratory data available in the sources for cylindrical particles were compared. The results showed compatibility between the results of modeling and laboratory data in the sources. Also, for solid-gas reactions for a given time when each of the resistances alone controls the rate of the CR, the results show that when the AL resistance controls the reaction rate, the conversion rate is more than the other

resistances. The results show that two curves including the GFL resistance curve and the CR resistance curve are the same, and both curves match each other because the conversion rate equations are the same.

This study also showed that in solid-gas reactions, the resistance of layers alone or their combination is significant in reaction rate control. However, with the advancement of the CR and further particle conversion, the resistances' relative importance, including the GFL, the AL resistance, and the CR resistance, will vary.In solid-gas reactions, the GFL resistance remains unchanged when the particle size remains constant during the reaction.

In solid-fluid reactions, the CR resistance increases with decreasing unreacted particle surface area. The AL resistance at the beginning of the reaction is zero because there is no ash yet. However, as the reaction advancement, the AL thickness increases, and the AL resistance becomes essential. Therefore, it is logical that the study of the rate of solid-gas reactions should not use only one resistance and use a combination of resistances.

Acknowledgments

Nomenclature

a	Length of flat plate particle (m)
a_i	Stoichiometry coefficients
C_{Ag}	Gas-phase concentration A (mole/m^3)
C_{As}	Concentration of component *A* on the non-reactive core surface (mole/m^3)
E	The exit age distribution of the solids in the reactor
F	Total feed moles (mol)
L	Half thickness of particle (m)
L_c	Half thickness of unreacted particle (m)
k_g	Mass transfer coefficient
Mw	Molecular weight (g/gmole)
n_B	Mole number B in particle (mole)
N_B	Solid moles number (mole)
ρ_B	Solid molar density (mole/m^3)
x_B	Solid conversion
$\overline{X_B}$	Average conversion of solid B
S_{ex}	Particle external surface (m^2)
S_B	Surface of particle (m^2)
t	Time of reaction (s)
τ	Complete conversion time for solid particle B (S)
$\bar{t}$	Mean residence time (s)
V_B	Particle Volume (m^3)

Symbols

AL	Ash layer
CR	Chemical reaction
GFL	Gas film layer
PCM	Progressive-conversion model
SCM	shrinking core model

References

[1]   Ebrahim HA, Jamshidi E. Kinetic study of zinc oxide reduction by methane. Chemical Engineering Research and Design. 2001 Jan 1;79(1):62-70.

[2]   Kimura S. Oxidation kinetics of polycrystalline zinc sulfide grains. AIChE journal. 1989 Feb;35(2):339-42.

[3]   Efthimiadis EA, Sotirchos SV. Reactivity evolution during sulfidation of porous zinc oxide. Chemical engineering science. 1993 Jan 1;48(5):829-43.

[4]   Delikouras EA, Perlmutter DD. Combined effects of mass transfer and inaccessible porosity in gasification reactions. AIChE journal. 1993 May;39(5):829-36.

[5]   Lozano-Castello D, Cazorla-Amoros D, Linares-Solano A. Powdered activated carbons and activated carbon fibers for methane storage: a comparative study. Energy & fuels. 2002 Sep 18;16(5):1321-8.

[6]   Bai D, Zhu JX, Jin Y, Yu Z. Simulation of FCC catalyst regeneration in a riser regenerator. Chemical Engineering Journal. 1998 Dec 2;71(2):97-109.

[7]   Denbigh, KG, Beverley, GSG. The Oxidation of Zinc Supplied Spheres in an Air Stream. Trans. Inst. Chem. Engr. 1962; 40: 23-34.

[8]   Szekely J, Evans JW, Sohn HY. Gas-Solid Reactions. Academic Press. 1976.

[9]   Beveridge GS, Goldie PJ. Effectiveness factors and instability in non-catalytic gas-solid reactions. The effect of solid heat capacity, Chemical Engineering Science. 1968 Aug 1;23(8):913-29.

[10]   SK Bhatia, DD Perlmutter, A random pore model for fluid–solid reactions. I. Isothermal, kinetic control, AIChE Journal. 1980 May;26(3):379-86.

[11]   Levenspiel O. Chemical reaction engineering. John Wiley & Sons;1999.

[12]   Rodriguez F, Revenga J, Tijero J. Study of anthraquinone reaction with sodium sulphide. The Chemical Engineering Journal and the Biochemical Engineering Journal, 1995;63:37-43.

[13]   Noorman S, Gallucci F, van Sint Annaland M, Kuipers JA. A theoretical investigation of CLC in packed beds. Part 1: Particle model. Chemical Engineering Journal. 2011 Feb 15;167(1):297-307.

[14]   Yagi S, Kunii D. Studies on combustion of carbon particles in flames and fluidized beds. InSymposium (international) on Combustion. 1955 Jan 1;5(1):231-244.

[15]   Levenspiel O. Chemical Reaction Engineering. John Wiley and Sons, 1962.

[16]   Kawasaki E, Sanscrainte, J, Walsh, J. Kinetics of Reduction of Iron Oxide with Carbon Monoxide and Hydrogen. AIChE Journal.1962; 8(1): 48-52.

[17]   Ishida M, Wen CY, Comparison of Kinetic and Diffusional Models for Solid-Gas Reactions. AIChE Journal. 1968 Mar;14(2):311-7.

[18]   Szekely J, Evans JW. A structural model for gas—solid reactions with a moving boundary. Chemical Engineering Science. 1970 Jan 1;25(6):1091-107.

[19]   Ramachandran PA, Smith JM. A Single Pore Model for Gas-Solid Non-Catalytic Reactions. AIChE Journal.1977; 23(3): 353-361.

[20]   Valipour H, Transactions C. Chemistry and Chemical Engineering. 2009;16(2):108-124.

[21]   Rashidi H, Ebrahim HA, Dabir B. Reduction kinetics of nickel oxide by methane as reducing agent based on thermogravimetry. Thermochimica acta. 2013 Jun 10;561:41-8.

[22]   Lv Z, Dang J. Mathematical modeling of the reaction of metal oxides with methane. RSC Advances. 2020;10(19):11233-43.

[23]   Tsinontides SC, Jackson R. The mechanics of gas fluidized beds with an interval of stable fluidization. Journal of Fluid Mechanics. 1993 Oct;255:237-74.

[24]   Ebrahimi AA, Ebrahim HA, Jamshidi E. Solving partial differential equations of gas–solid reactions by orthogonal collocation. Computers & Chemical Engineering. 2008 Aug 22;32(8):1746-59.

[25]   Movagarnejad K, Sohrabi M, Kaghazchi T, Vahabzadeh F. A model for the rate of enzymatic hydrolysis of cellulose in heterogeneous solid–liquid systems. Biochemical Engineering Journal. 2000 Feb 1;4(3):197-206.